ULTRASONIC TRANMISSION THROUGH MULTIPLE-SUBLATTICE SUBWAVELENGTH HOLES ARRAYS

Héctor Estrada[1,2], Vicente Gómez-Lozano[1], Antonio Uris[1,3], Pilar Candelas[1], Francisco Belmar[1], Francisco Meseguer[1,2]

[1]Centro de Tecnologías Físicas, Unidad Asociada ICMM-CSIC/UPV,

Edificio 8B Bloque K, Ciudad Politécnica de la Innovación, Universidad Politécnica de Valencia, 46022 Valencia, Spain

Phone: 34.963877528; Fax: 34.963879525; E-mail: auris@fis.upv.es

[2] Instituto de Ciencia de Materiales de Madrid (CSIC), Cantoblanco, 28049 Madrid, Spain

[3] Corresponding author.

ABSTRACT

The ultrasonic transmission through plates perforated with 2x2 or 3x3 square array of subwavelength holes per unit cell are studied by numerical simulations. Calculations are obtained by means of a theoretical model under the rigid-solid assumption. It is demonstrated that when the inter-hole distance within the unit cell is reduced, appear new transmission dips resulting from Wood anomalies that have influence on the second and the third order Fabry-Perot peak. When the inter-hole distance within the unit cell is reduced, the transmission spectrum of the multiple-sublattice holes arrays tends to the transmission spectrum of a plate perforated with only one hole in the unit cell.

Keywords: Subwavelength, multiple-sublattice, hole array, ultrasonic transmission.

1. INTRODUCTION

In recent years, the extraordinary optical transmission through metallic membranes perforated with subwavelength hole arrays [1] has attracted considerable attention. One important characteristic of periodic subwavelength hole arrays drilled on a metallic membrane is that they transmit much light than expected from Bethe's theory [2]. A lot of discussion have raised in the literature for elucidating the mechanisms involved in the extraordinary optical transmission. Martin-Moreno et al. [3] and Barnes et al. [4] attributed this effect to surface plasmon resonances, Cao et al. [5] to cavity resonances, Porto et al. [6] to waveguide resonance and Takakura [7] to dynamical diffraction. Inspired by the studies in electromagnetic waves, investigation has been extended to acoustic waves, emphasizing the similarities between both cases, but taking into account the intrinsic differences between them, namely: acoustic waves can be transmitted through a single subwavelength hole [8] and, depending on the impedance contrast between fluid and solid, can penetrate into solid [9]. The so-called extraordinary acoustic transmission was reported experimentally by Lu et al. [10] and Hou et al. [11] for slit and hole arrays, respectively, and theoretically by Christiansen et al. [12]. It is widely accepted that Fabry-Perot resonances are the main responsible for extraordinary acoustic transmission. Estrada et al. [13] have shown that water-inmersed aluminium plates perforated with periodic subwavelength hole arrays exhibit not only full transmission peaks, but also extraordinary ultrasound screening over a frequency region around Wood anomaly [14]. It was also demonstrated that the position and width of transmission peaks and dips can be tuned by changing the filling fraction of holes [15] and the lattice geometry [16]. Estrada et al. [9] also demonstrated that Lamb and Scholte-Stoneley modes are strongly coupled to Fabry-Perot and lattice resonances in a water-inmersed perforated plate.

The aim of this paper is to study theoretically the interaction between the different resonances when multiple subwavelength holes arrays are arranged in a unit cell. The ultrasound transmission through plates perforated is calculated when the individual unit cells comprise 2x2 or 3x3 square array of subwavelength holes. The spacing between holes in unit cell is varied to examine its effect on the transmission spectra.

2. BASIC THEORY

Consider a plane ultrasound wave incident on a rigid plate of thickness h drilled with P cylindrical holes of radius r_0 in positions determined by their centres $\vec{r}_i$, as schematically shown in Figure 1.

Assuming an incident plane wave $\phi_0(\vec{r}) = e^{i(\vec{k}_0 \cdot \vec{r} - \omega t)}$, the reflected and the transmitted ultrasound pressure fields can be expressed in terms of plane waves expansion. For simplicity, time harmonic excitation is assumed, thus the time component $e^{-i\omega t}$ can be omitted. By using the rigid-solid assumption, that is, there is no field inside the solid, the pressure field in the three regions can be written as follows [17,18]:

$$\phi_I(\vec{r}) = \phi_0(\vec{r}) + \phi_R(\vec{r}) = e^{i(\vec{Q}_0 \cdot \vec{r}_\parallel - q_0 z)} + \iint \beta^+(\vec{Q}) e^{i(\vec{Q} \cdot \vec{r}_\parallel + qz)} d^2\vec{Q}, \tag{1}$$

$$\phi_{II}(\vec{r}) = \begin{cases} \sum_{i=1}^{P} \sum_{m=0}^{\infty} \sum_{n=1}^{\infty} J_m\left(Q_{mn}^i \left|(\vec{r} - \vec{r}_i)_\parallel\right|\right) e^{im\varphi_i} \Psi_{mn}^i(z) & if \quad |\vec{r} - \vec{r}_i| \le r_0 \\ 0 & otherwise \end{cases}, \tag{2}$$

$$\phi_{III}(\vec{r}) = \iint \beta^-(\vec{Q}) e^{i(\vec{Q} \cdot \vec{r}_\parallel - q(z+h))} d^2\vec{Q}, \tag{3}$$

where $\vec{k}_0 = (\vec{Q}_0, q_0)$, $k_0 = \omega/c$, $q = \sqrt{k_0^2 - Q^2}$, $q_{mn}^i = \sqrt{k_0^2 - Q_{mn}^{i\,2}}$, $J_m(...)$ is the Bessel

function of the first kind and order m, and $\Psi^{i}_{mn}(z)$ is defined as

$$\Psi^{i}_{mn}(z) = \alpha^{i+}_{mn}\, e^{iq^{i}_{mn}z} + \alpha^{i-}_{mn}\, e^{-iq^{i}_{mn}z} .$$

As the plate is treated as a perfect rigid solid, zero normal velocity at the hole walls is assumed and the polar eigenfunctions inside the hole must satisfy $J'_m\left(Q^{i}_{mn} r_0\right) = 0$.

Repeating the P holes periodically throughout the whole plate, they can be considered as a lattice basis with a unit-cell area S and defined by the vectors $(\vec{a}_1, \vec{a}_2)$. In this way, the coefficients $\beta^{\pm}\left(\vec{Q}\right)$ can be expanded as Fourier series, giving discrete expressions [19] for equations (1) and (3)

$$\phi_I(\vec{r}) = 2e^{i\left(\vec{Q}_0\cdot\vec{r}_{\parallel}\right)}\cdot\cos\left(q_0\cdot z\right) + \sum_{\vec{G}} \beta^{+}_{\vec{G}}\, e^{i\left(\vec{Q}_{\vec{G}}\cdot\vec{r}_{\parallel} + q_{\vec{G}}z\right)} , \tag{4}$$

$$\phi_{III}(\vec{r}) = \sum_{\vec{G}} \beta^{-}_{\vec{G}}\, e^{i\left(\vec{Q}_{\vec{G}}\cdot\vec{r}_{\parallel} - q_{\vec{G}}(z+h)\right)} , \tag{5}$$

where $\vec{Q}_{\vec{G}} = \vec{Q}_0 + \vec{G}$, $\vec{G}$ is the reciprocal lattice vector of $(\vec{a}_1, \vec{a}_2)$, and $q_{\vec{G}} = \sqrt{k_0^2 - Q_{\vec{G}}^{\,2}}$. The objective is to determine the coefficients $\beta^{+}_{\vec{G}}, \beta^{-}_{\vec{G}}, \alpha^{i+}_{mn}$ and α^{i-}_{mn} by imposing the continuity of the normal velocity at $z = 0$ and $z = -h$ and imposing pressure continuity at $z = 0$ and $z = -h$. Once $\alpha^{\pm}_{mn}$ and $\beta^{\pm}_{\vec{G}}$ are obtained, the ultrasound power transmission coefficient can be calculated from the ultrasound power radiated by an infinite plate [20] ,

$$\tau = \frac{\Pi_T(\omega)}{\Pi_0(\omega,\theta,\varphi)} = \sum_{\vec{G}} Re\left\{\frac{q_{\vec{G}}}{q_0}\right\}\left|\beta^{-}_{\vec{G}}\right|^2 .$$

3. NUMERICAL RESULTS AND DISCUSSION

The numerical calculations are made considering 2x2 and 3x3 multiple-sublattice holes arrays placed in water. In each 2x2 and 3x3 squared holes arrays considered, the period of the unit cell, a, is fixed and the inter-hole distance within the unit cell, p, is varied. The values of p considered are a/2, 10a/24 and a/3 in the 2x2 squared holes arrays and a/3, 3a/10 and 7a/30 in the 3x3 squared holes arrays. All the samples considered have a thickness h = 3 mm and a fixed hole filling fraction 0.25. The period of the unit cells, a, is 5 mm. Multiple-sublattice hole unit cells considered are showed in Figure 2. The transmitted ultrasound power coefficient, τ, as a function of frequency, f, in the fluid at normal incidence of the 2x2 multiple-sublattice holes arrays is calculated separately for samples with the inter-hole distance within the unit cell a/2, 10a/24 and a/3 and are depicted in Figures 3(a)-(c), respectively. The sample with the inter-hole distance within the unit cell a/2 (Figure 3(a)) corresponds to a square lattice holes arrays with period a/2 = 2.5 mm. The full transmission peaks observed correspond to Fabry-Perot resonances of the holes cavities and modulated by the interaction among holes and the minimum transmission dips at frequencies around 590 kHz and 840 kHz correspond to the manifestation of Wood anomalies. The Wood anomaly for normal incidence is given by $\frac{\omega}{c} = \sqrt{\left(\frac{2\pi m}{l}\right)^2 + \left(\frac{2\pi n}{l}\right)^2}$, where l is the array period, n,m are called Miller indices and c is the speed of ultrasound in water. When the inter-hole distance within the unit cell is reduced to 10a/24 (Figure 3(b)), new transmission dips appears resulting from Wood anomalies corresponding to the period of the unit cell. The Wood minima associated to the period of the unit cell (296 kHz and 420 kHz) have effect in the appearance of the second order transmission peak while the first order Fabry-Perot peak is invariable. The calculated results for the sample with the inter-hole distance within the unit cell 7a/30 are shown in Figure 3(c). The prevalence of the first

order Fabry-Perot transmission peak is evident, while the amplitude of the second order transmission peak is reduced at half due the interplay with Wood anomaly minima associated with the period of the unit cell, which are more obvious. Figure 3(d) shows transmitted ultrasound power coefficient of a sample with one hole within the unit cell with period a = 5 mm and a hole filling fraction 0.25. The full transmission peak observed correspond to the first order Fabry-Perot holes resonances and the minimum transmission dips correspond to the manifestation of Wood anomalies. The existence of Wood anomalies is related to the geometrical structure factor of the lattice. Thus, Figures 4(a)-(d) are obtained by appliying a two-dimensional Fourier transform to the real space lattice. It can be clearly seen that for p values of 10a/24 (Fig.4(b)), a/3 (Fig.4(c)), and single hole (Fig.4(d)), the structure factor is the same and only the relative amplitude between the peaks changes.

In the case of the 3x3 multiple-sublattice hole arrays samples, the transmitted ultrasound power coefficient, τ, as a function of frequency, f, at normal incidence is calculated separately for the case where the inter-hole distance within the unit cell is a/3, 3a/10 and 7a/30 and are depicted in Figures 5(a)-(c), respectively. Figure 5(a) shows transmitted ultrasound power coefficient of the sample with the inter-hole distance within the unit cell a/3, that corresponds to a square lattice holes arrays with period a/3 = 1.67 mm. Like in the 2x2 case, the full transmission peaks observed correspond to Fabry-Perot holes resonances, but a new Fabry-Perot resonance arises due to the addition of extra holes in the unit cell. The minimum transmission dips at frequencies around 880 kHz and 1260 kHz correspond to the manifestation of Wood anomalies. When the inter-hole distance within the unit cell are reduced to 3a/10 (Figure 5(b)) and to 7a/30 (Figure 5(c)) appear new transmission dips resulting from Wood anomalies corresponding to the period of the unit cell. The effect of Wood

minima associated with the period of the unit cell increase their effect in the appearance of the second and third order transmission peaks as distance of the holes within the unit cell are reduced while the frequency of the first order Fabry-Perot peak remains invariable. As showed in 2x2 case Figure 5(d) shows transmitted ultrasound power coefficient of a sample with one hole within the unit cell with period a = 5 mm and a hole filling fraction 0.25. The geometrical structure factor for the 3x3 multiple-sublattice hole array samples shows the same behaviour observed in the 2x2 case, as can be seen in Figures 6(a)-(d). From Figures 3(a)-(d) and Figures 5(a)-(d) it can observed that the transmission spectrum of the multiple-sublattice holes arrays tends to one with only one hole in the unit cell. One remarkable feature shown in Figure 5(c) is that the first order Fabry-Perot resonance peak splits into two peaks. The transmission dip that gives rise to the splitting of the first order Fabry-Perot resonance peak arises from the interference between holes [21]. When the holes have the same area, the coupling between them is strong and when the phase difference between holes in a unit cell approaches π, as shown in Figure 7(a)-(c), the interference between them lead a destructive interference. In addition to the π phase shift linked to the resonance splitting of the first Fabry-Perot mode, other phase shift peaks can be observed at higher frequencies in Figures 7(b) and 7(c). However, these shift peaks are highly influenced by the lattice structure factor (see Figure 6(b), (c)). Thus, as the structure factor for both lattices is roughly the same, the difference observed in the transmission spectra can be attributed to the inter-hole distance p as it clearly modifies the inter-hole interaction.

4. CONCLUSIONS

Ultrasound transmission through periodically perforated plates with multiple-sublattice holes arrays has been studied theoretically. Ultrasound transmission spectrums were

calculated by using a model in the rigid-solid limit. The results show that, in both 2x2 and 3x3 squared holes arrays, when the inter-hole distance within the unit cell is reduced, appear new transmission dips resulting from Wood anomalies corresponding to the period of the unit cell and the period of the holes within the unit cell. The Wood minima associated with the period of the unit cell have effect in the appearance of the second order transmission peak while the first order Fabry-Perot peak is invariable. For the 3x3 squared holes arrays the first order Fabry-Perot resonance peak splits into two when the phase difference between holes in a unit cell approach π. As the inter-hole distance within the unit cell is reduced, the transmission spectrum of the multiple-sublattice holes arrays tends to one with only one hole in the unit cell. These results are expected to have applications in ultrasonic filters.

Acknowledgments

This work has been supported by the Spanish MICINN (MAT2010-16879), Generalitat Valenciana (PROMETEO 2010/043) and Universidad Politecnica de Valencia (PAID-06-10-1839). H. E. acknowledges the support of CSIC-JAEpredoc scholarship.

REFERENCES

[1] T.W. Ebbesen, H. J. Lezec, H. F. Ghaemi, T. Thio and P.A. Wolf, Extraordinary optical transmission through sub-wavelength hole arrays Nature (London) 391 (1998) 667-669.

[2] H.A. Bethe, Theory of diffraction by small holes, Phys. Rev. 66 (7-8) (1944) 163-182.

[3] L. Martin-Moreno, F. J. Garcia-Vidal, H. J. Lezec, K. M. Pellerin, T. Thio, J. B. Pendry, T. W. Ebbesen, Theory of extraordinary optical transmission through subwavelength hole arrays, Phys. Rev. Lett. 86 (6) (2001) 1114-1117.

[4] W. L. Barnes, A. Dereux, T. W. Ebbesen, Surface plasmon subwavelength optics, Nature 424 (2003) 824-830.

[5] Q. Cao and P. Lalanne, Negative role of surface plasmons in the transmission of metallic gratings with very narrow slits, Phys. Rev. Lett. 88, (2002), 057403-057406.

[6] J. A. Porto, F. J. Garcia-Vidal and J.B. Pendry, Transmission resonances on metallic gratings with very narrow slits, Phys. Rev. Lett. 83 (1999) 2845-2848.

[7] Y. Takakura, Optical resonance in a narrow slit in a thick metallic screen , Phys. Rev. Lett. 86 (2001), 5601-5604.

[8] F.J. Garcia de Abajo, H. Estrada and F. Meseguer, Diacritical study of light, electrons and sound scattering by particles and holes, New J. Phys. 11, (2009), 093013.

[9] H. Estrada, F. J. Garcia de Abajo, P. Candelas, A. Uris, F. Belmar, F. Meseguer, Angle-dependent ultrasonic transmission through plates with subwavelength hole arrays, Phys. Rev. Lett. 102 (14) (2009) 144301-144304.

[10] M. Lu, X. Liu, L. Feng, J. Li, C. Huang, Y. Chen, Y. Zhu, S. Zhu and N. Ming, Extraordinary acoustic transmission through a 1D grating with very narrow apertures Phys. Rev. Lett. 99 (2007), 174301-174301.

[11] B. Hou, J. Mei, M. Ke, W. Wen, Z. Liu, J. Shi and P. Sheng, Tuning Fabry-Perot resonances via diffraction evanescent waves Phys. Rev. B 76 (2007), 054303-054309

[12] J. Christensen, L. Martin-Moreno, F.J. Garcia-Vidal, Theory of resonant acoustic transmission through subwavelength apertures, Phys. Rev. Lett. 101, 014301, (2008) .

[13] H. Estrada, P. Candelas, A. Uris, F. Belmar, F. J. Garcia de Abajo, F. Meseguer, Extraordinary sound screening in perforated plates, Phys. Rev. Lett. 101 (8) (2008) 084302-084305.

[14] R.W. Wood, On a remarkable case of uneven light in a diffraction grating, Phil. Mag. 4, (1902) 396-402.

[15] H. Estrada, P. Candelas, A. Uris, F. Belmar, F. Meseguer, F. J. Garcia de Abajo, Influence of the hole filling fraction on the ultrasonic transmission through plates with subwavelength aperture arrays, Appl. Phys.Lett. 93 (1) (2008) 011907-011909.

[16] H. Estrada, P. Candelas, A. Uris, F. Belmar, F. J. Garcia de Abajo, F. Meseguer, Influence of lattice symmetry on ultrasound transmission through plates with subwavelength aperture arrays, Appl. Phys. Lett. 95 (5) (2009) 051906-051906.

[17] H. Estrada, P. Candelas, A. Uris, F. Belmar, F. J. Garcia de Abajo, F. Meseguer, Sound Transmission through perforated plates with subwavelength hole arrays: A rigid-solid model, Wave Motion 48 (3) (2010), 235-242.

[18] H. Estrada, V. Gómez-Lozano, A. Uris, P. Candelas, F. Belmar, F. Meseguer, Sound transmissión through plates perforated with two periodic subwavelength hole arrays, J. Phys.: Condens. Matter 23 (2011), 135401.

[19] Charles Kittel. Introduction to Solid State Physics. John Wiley & Sons, 7 th edition, 1996

[20] Earl G. Williams. Fourier Acoustics: sound radiation and nearfield acoustical holography. Academic Press, 1999.

[21] Z. Liu and G. Jin, Resonant acoustic transmission through compound subwavelength hole arrays: the role of phase resonances, J. Phys: Condens. Matter 21 (2009) 445401.

FIGURES CAPTIONS

Figure 1. Schematic representation of the (a) "xz" plane and (b) "xy" plane of the unit-cell. Gray regions correspond to the rigid solid whereas the surrounding fluid is divided in 3 regions as indicated by the labels in a). The vector $\left(\vec{r}-\vec{r}_i\right)_{\|}$ in (b) represents the projection over the z=0 plane of the vector defined from the centre of each hole to the appropriate points in the fluid region 2.

Figure 2. Diagrammatic sketch of the unit cells of the samples considered.

Figure 3. Transmitted ultrasound power coefficient of the 2x2 multiple-sublattice holes arrays with the three different periodicities of the holes within the unit cell: a) a/2, b) 10a/24 and c) a/3, d) sample with one hole within the unit cell with period a and hole filling fraction 0.25, where a = 5 mm.

Figure 4. Structure factor of the 2x2 multiple-sublattice holes arrays with the three different inter-hole distances within the unit cell: a) a/2, b) 10a/24 and c) a/3, d) sample with one hole within the unit cell with period a and hole filling fraction 0.25, where a = 5 mm.

Figure 5. Transmitted ultrasound power coefficient of the 3x3 multiple-sublattice holes arrays with the three different periodicities of the holes within the unit cell: a) a/3, b) 3a/10 and c) 7a/30, d) sample with one hole within the unit cell with period a and hole filling fraction 0.25, where a = 5 mm.

Figure 6. Structure factor of the 3x3 multiple-sublattice holes arrays with the three different inter-hole distances within the unit cell: a) a/3, b) 3a/10 and c) 7a/30, d) sample with one hole within the unit cell with period a and hole filling fraction 0.25, where a = 5 mm

Figure 7. Phase differences of the fields between the central and the extreme holes (black) and between the central and the middle holes (gray) on the 3x3 multiple-sublattice holes arrays. The periodicities of the holes within the unit cell are: a) a/3, b) 3a/10 and c) 7a/30, where a = 5 mm.

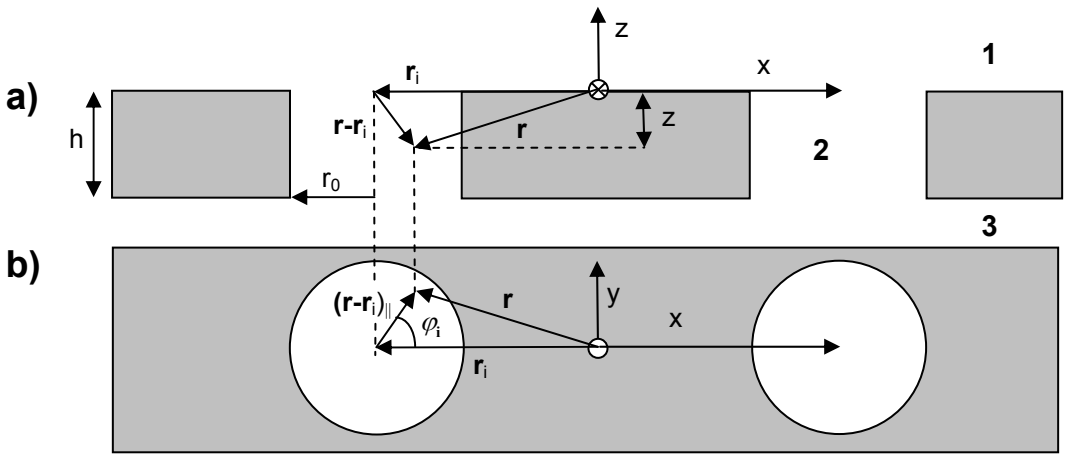
a)
b)
z
x
1
2
3
h
$\mathbf{r}_i$
$\mathbf{r}$-$\mathbf{r}_i$
$\mathbf{r}$
z
r_0
y
x
$(\mathbf{r}-\mathbf{r}_i)_{\parallel}$
φ_i
$\mathbf{r}_i$

Figure 1

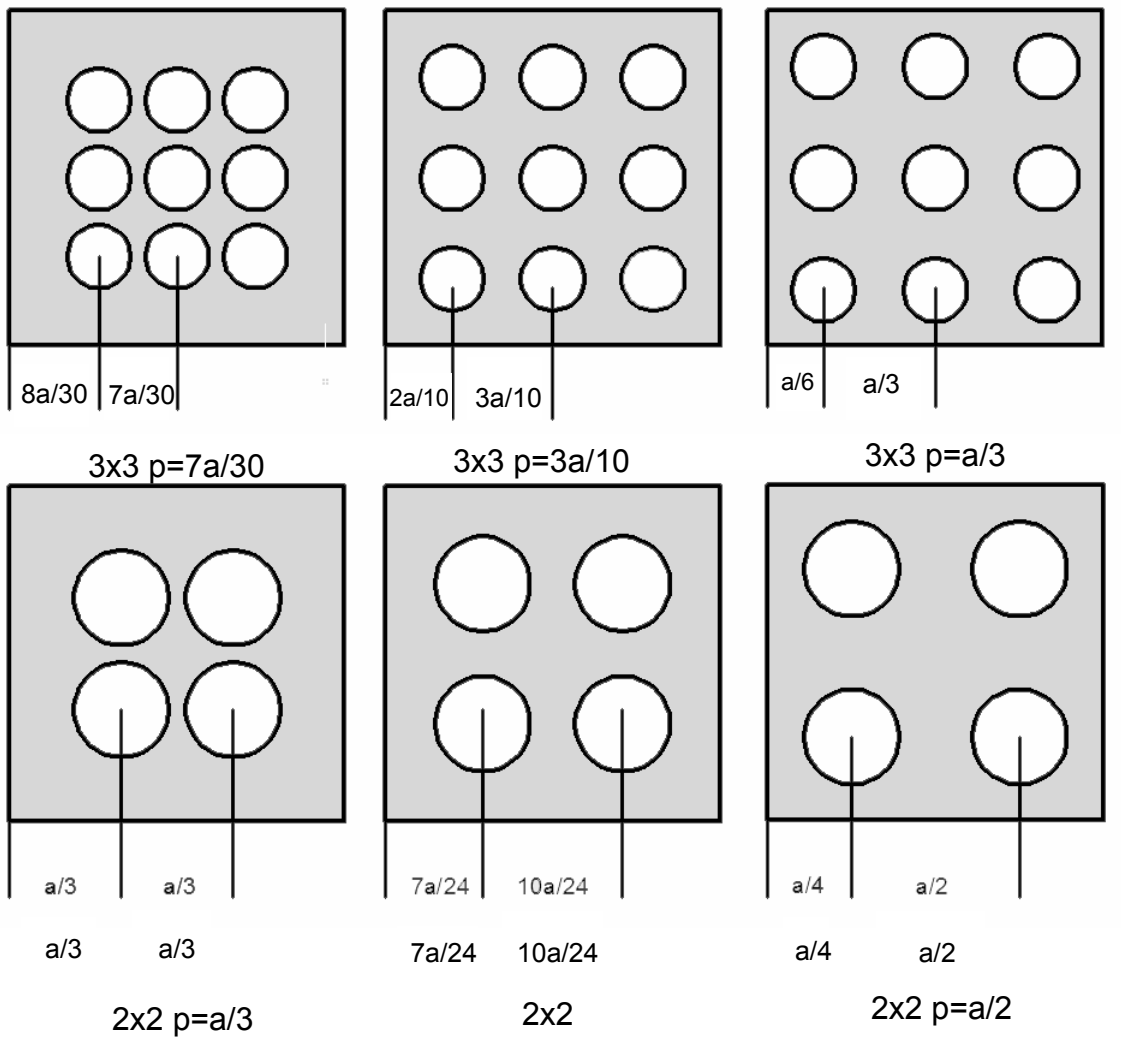
8a/30
7a/30
3x3 p=7a/30
2a/10
3a/10
3x3 p=3a/10
a/6
a/3
3x3 p=a/3
a/3
a/3
a/3
a/3
2x2 p=a/3
7a/24
10a/24
7a/24
10a/24
2x2
a/4
a/2
a/4
a/2
2x2 p=a/2

Figure 2

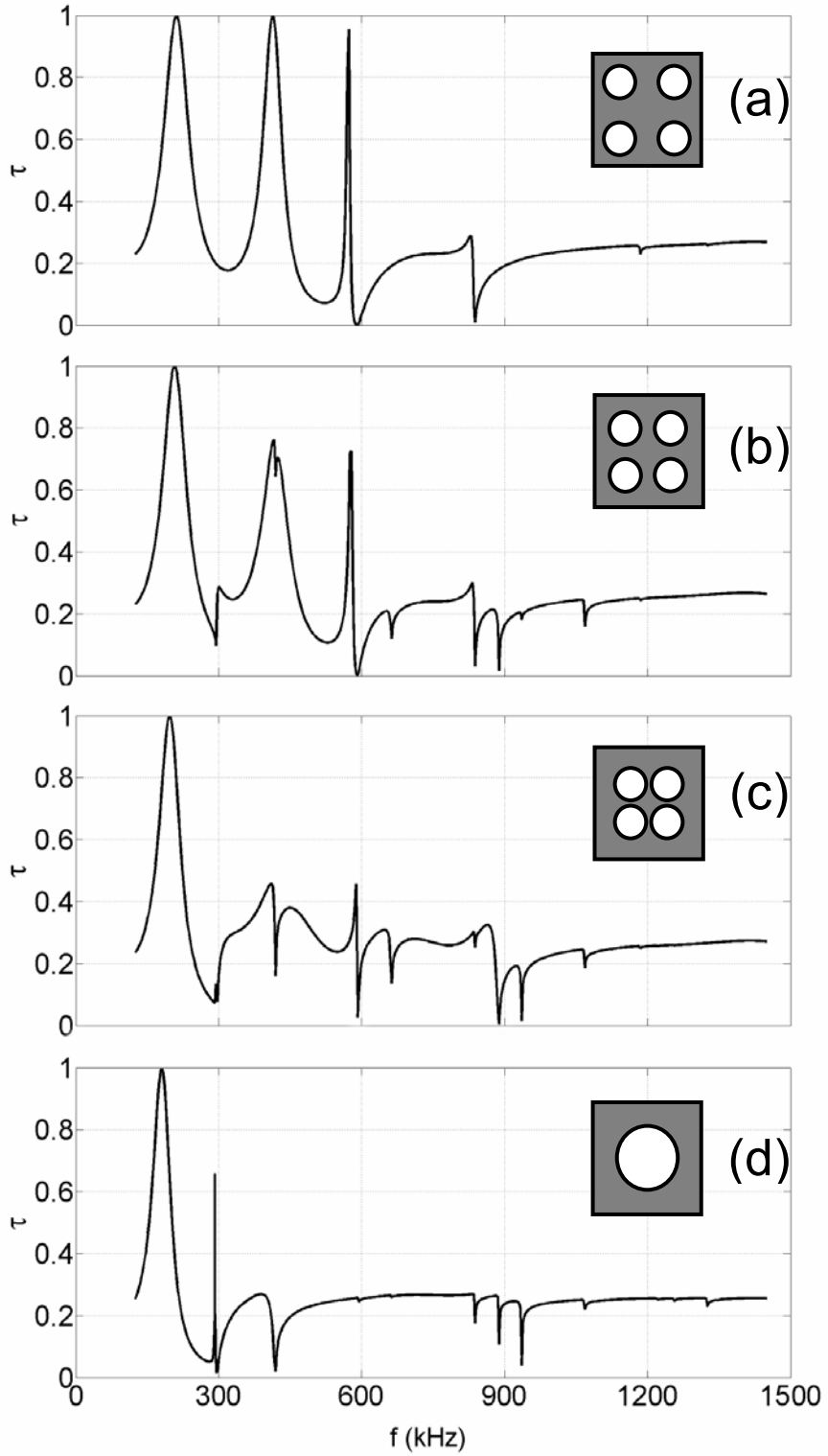

Figure 3

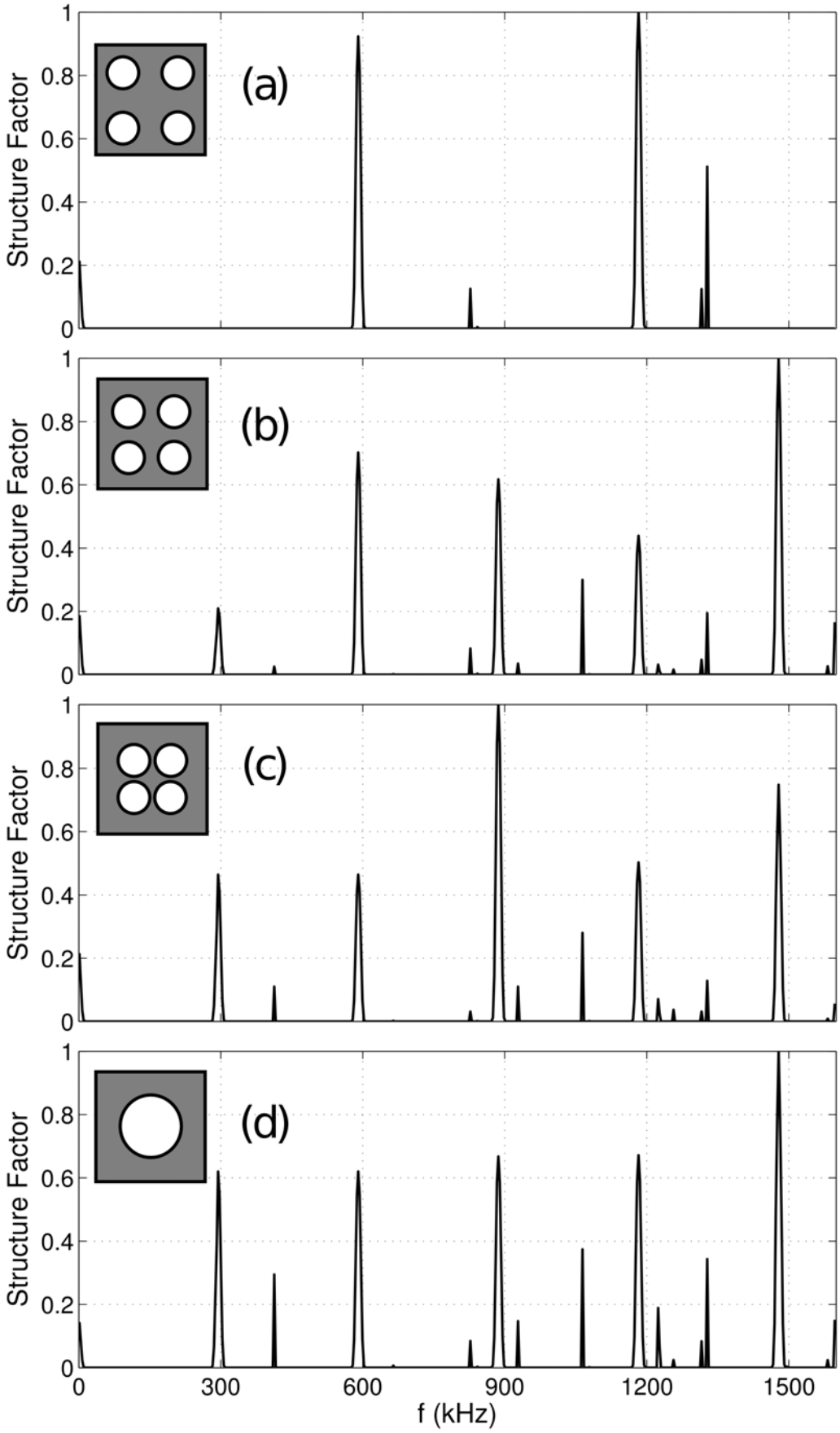
(a)
(b)
(c)
(d)
Structure Factor
0
0.2
0.4
0.6
0.8
1
0
300
600
900
1200
1500
f (kHz)

Figure 4

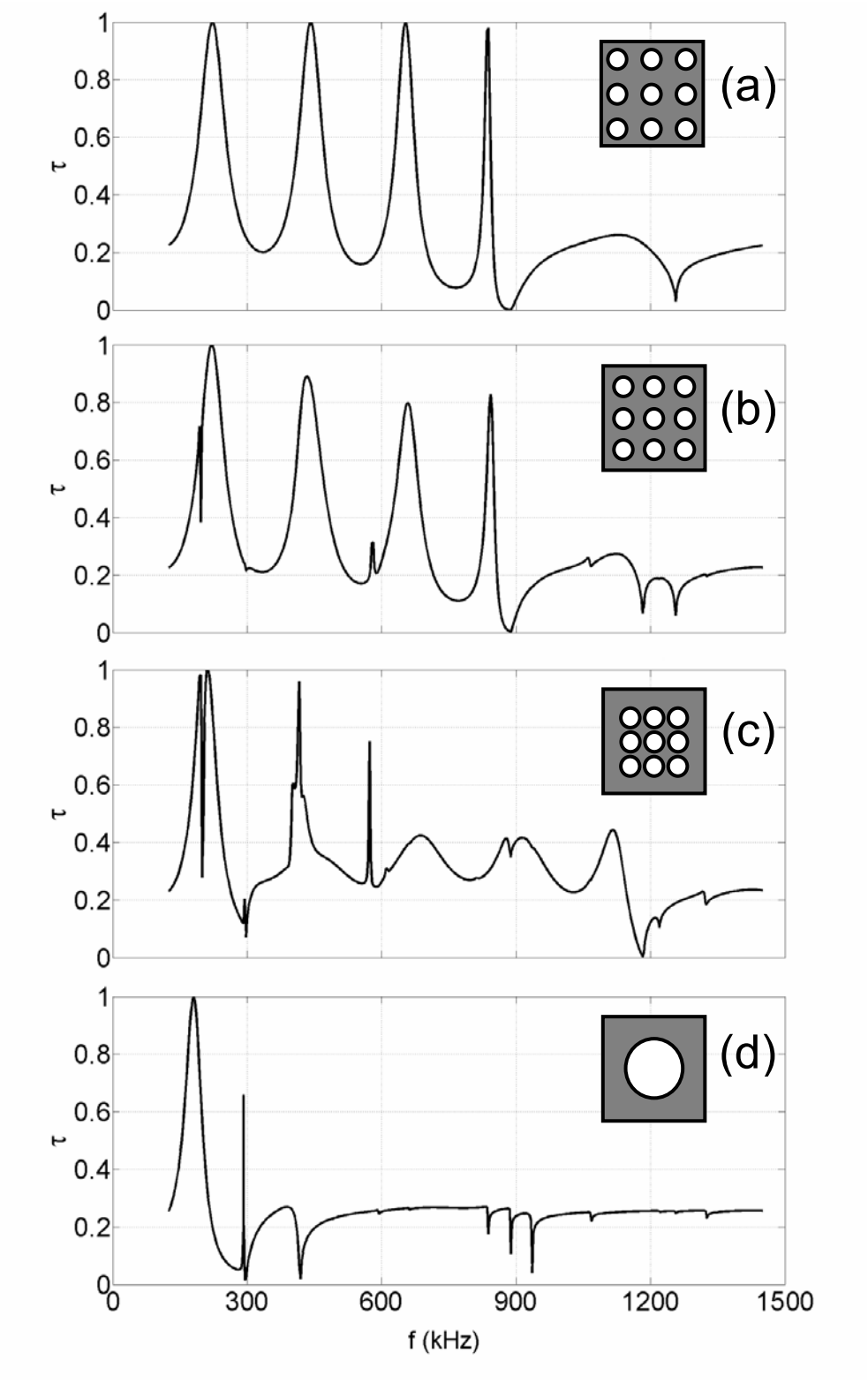

Figure 5

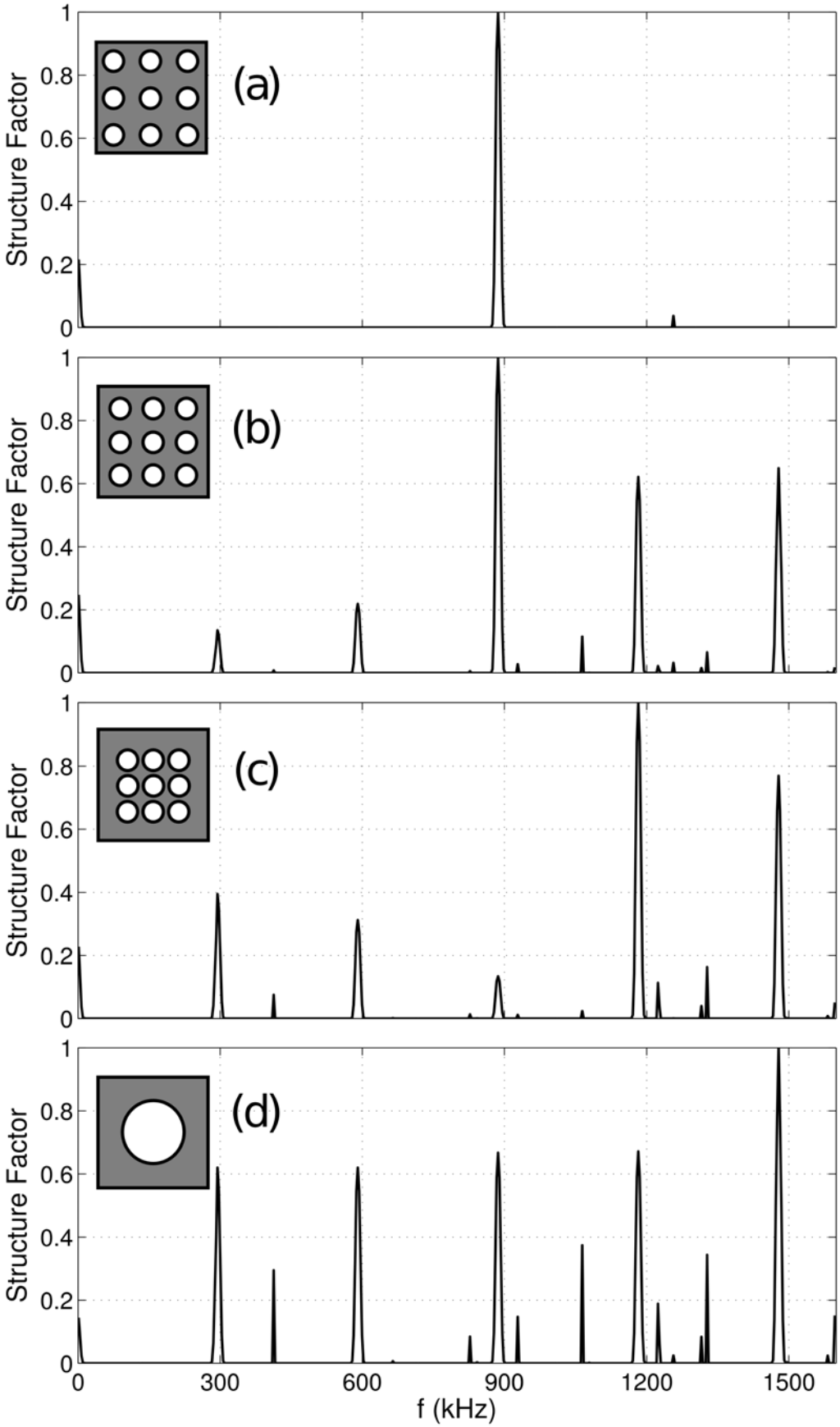
(a)
(b)
(c)
(d)
Structure Factor
0
0.2
0.4
0.6
0.8
1
0
300
600
900
1200
1500
f (kHz)

Figure 6

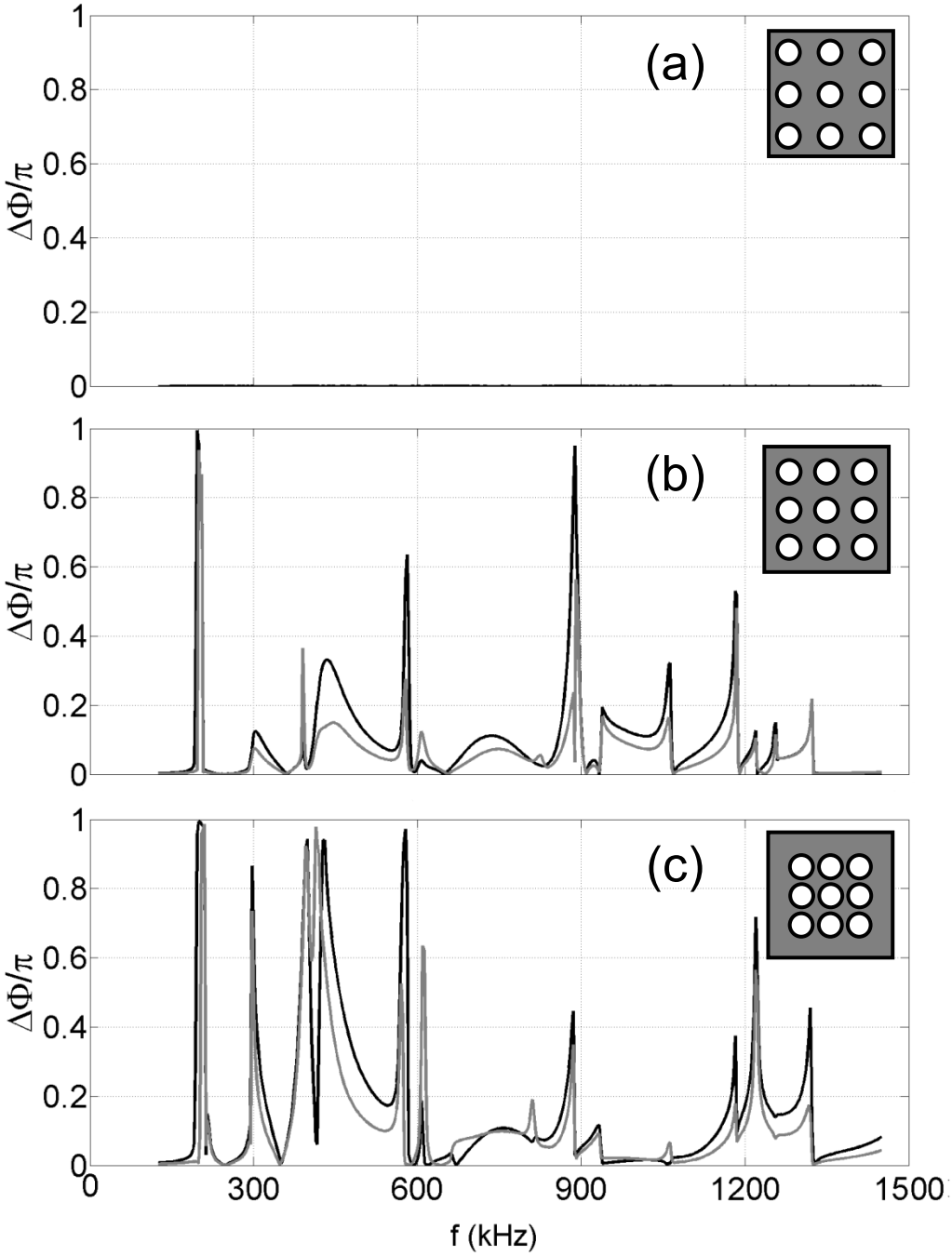

Figure 7